**<Final Report: EEE4610-01>**

# Frequency Stability of Different GFM-GFL Ratios in Zero-Inertia Grids

Dela Rosa Joshua Gabriel
School of Electrical and Electronic Engineering
College of Engineering
Yonsei University

<Final Report: EEE4610-10>

# Frequency Stability of Different GFM-GFL Ratios in Zero-Inertia Grids

Report Advisor: Kyeon Hur

December 2023

Dela Rosa Joshua Gabriel
School of Electrical and Electronic Engineering
College of Engineering
Yonsei University

# CONTENTS

# ABSTRACT

## Frequency Stability of Different GFM-GFL Ratios in Zero-Inertia Grids

The challenge of integrating renewable energy sources to the power grid stems from its inherent lack of inertia to provide frequency support. GFLs mainly inject power into the grid as a current source while following the grid which inherently makes it unable to support grid during instabilities. GFMs on the other hand form their own voltage at its PCC (point of common coupling) hence are closer in nature to synchronous generators. To exploit this, GFMs are controlled to emulate synchronous generator characteristics via frequency droop and/or swing equation emulation. Despite promising characteristics, the grid at high penetration of IBRs or zero-inertia grids tend to have a different frequency characteristic. Related work shows that GFMs are unstable at supposedly strong grids and that GFL elements can still be utilized to support grid frequency at high penetration [4]. To further investigate GFL-GFM interactions, the student simulated different GFM to GFL ratios on the IEEE 14 bus grid with 100% IBRs as generators to determine frequency stability. Results show that a ratio of 4:1 result in consistent frequency responses when faced with disturbances such as load changes and faults.

---

Key words: GFM, GFL, Inertia, Frequency stability, Zero-inertia, high-penetration, duality

# I. INTRODUCTION

Integrating renewable energy sources in the power grid is becoming more imperative. However, the challenge of keeping the grid's frequency stable is a challenge as replacing synchronous generators reduces inertia [1]. Inertia from its large rotating masses keeps frequency stable during contingencies which reflects grid strength. Thus, lack of rotating masses by inverter-based resources (IBRs) hinders high penetration due to grid frequency stability issues [1].

Traditional IBRs in the form of *grid following inverters* (GFLs) primarily inject power based on *maximum power point tracking* (MPPT) while following the grid's voltage [2]. However, if contingencies arise, GFLs cannot fully support the grid frequency due to lack of inertia [2], [4], [5]. Additionally, GFLs follow the grid using *phase-locked loop* (PLLs) which makes it more susceptible to instabilities. Thus, a new form of IBRs called *grid forming inverters* (GFMs) form its own voltage and frequency reference, and does not follow the grid using a PLL which makes it less susceptible to grid instabilities [2]. Hence, GFMs are similar to traditional synchronous machines. To further exploit this characteristic, GFMs are controlled to emulate frequency droop and inertial response of synchronous machines to help support grid frequency.

However, in high and/or zero penetration grids, the grid characteristics deviate from traditional grids [3]. GFMs in supposedly stiff grids are unstable and that the SCR-based grid strength should be reconsidered [3], [4]. GFMs and GFLs also show duality and that benefits from both could be utilized to help support grid frequency [4], [5].

Therefore, I am enthused to investigate frequency stability of different GFM-GFL ratios in zero penetration grids with an aim to provide insights on how GFMs and GFLs in different ratios interact to support grid frequency stability during load changes and faults.

# II. BACKGROUND

## II.A Grid Frequency and Grid Inertia

Traditional power grids involve synchronous generators operating in lockstep and have large rotating masses which stores inertia. Inertia can be used as a temporary power source during disturbances which helps frequency stability which reflects grid strength [1]. Specifically, inertia allows time for system operators to apply necessary protocols to handle power imbalances disturbances such as load changes, faults, and loss of generators. However, as we transition to renewable energy sources using IBRs, the lack of large rotating masses reduces system inertia hence the frequency stability of the grid.

The importance of inertia is best understood through an analogy with a running bicycle. A bicycle will continue moving forward even if the cyclist stops pedaling. The energy stored in the rotation of the wheels allow it to move forward – slowing it down as more inertia and the cyclist must pedal again to regain speed. In the same way, for disturbances in the grid, such as a loss of generator, the stored inertia in the remaining machines would allow the grid to operate for a brief period of time. At this point, the system operators would be able to adjust the operating points or apply certain mechanisms to keep the grid stable and functioning.

Lack of inertia causes frequency instability. If for some reason, the frequency greatly deviates away from nominal (for instance drop below certain minimum), measures such as load shredding must be conducted to regain system frequency [1]. In high penetration grids, the lack of synchronous generators becomes an issue for frequency stability. This slows down integration of renewable energy sources to the grid.

## II.0 Preliminaries: Voltage Sourced Inverters and their Control

To understand how GFLs and GFMs work, a thorough study of voltage sourced converters (VSC) are conducted. A VSC is a type of converter wherein its DC side voltage does not change polarity while the direction of current determines the direction of average power flow. An example is the Half-bridge converter shown below in figure 1. Through the use of power electronics and pulse-width modulation (PWM), sinusoidal power can be delivered to and from an AC system. The VSC can also be configured to supply 3-phase power.

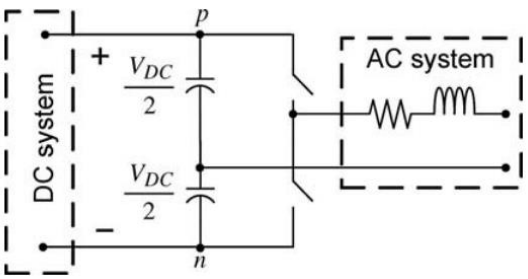


Figure 1: Single Phase Half-Bridge Converter

Control of VSC is based on the relationship between the AC-side current dynamics and the average voltage on the terminals of the converter which is described by the following equation. However, since the inputs of the system is not a step function nor a ramp but a sinusoid, the control of the VSC in three-phases is no easy task and creating a controller for three sinusoids can be demanding – worse, tracking sinusoids does not result in zero steady state errors. However, if analyzed in phasor form the controller design can be simplified.

$$\mathrm{L}\frac{di}{dt} + (R + r_{on})i = V_t - V_s$$

When a sinusoid is analyzed in phasor notation, only the magnitude and the angle of the sinusoid can be used as the signal for control. However, it is preferred to design controllers in Cartesian coordinates [VSC]. Hence, the real- and –imaginary axes of the phase are mapped in Cartesian plane. In this *αβ-frame* analysis, the number of sinusoids are reduced to two. However, since sinusoidal input tracking does not result in zero steady-state error, the inputs to the controller must be changed to a DC signal.

The *αβ-frame* technique can be refined to convert the controller design frame from a sinusoidal frame to DC frame. This can be done by letting the αβ-axes to rotate with the frequency of the phasor. In this way, the resulting magnitudes read by the axes remain constant. This control frame is called *dq-frame*. In this manner, the controller design for a sinusoidal input can be converted to a design for a DC controller. Figure 2 below shows the difference between *αβ-* and *dq-frame*s. Transformation to *dq-frame* is also called "Park Transformation".

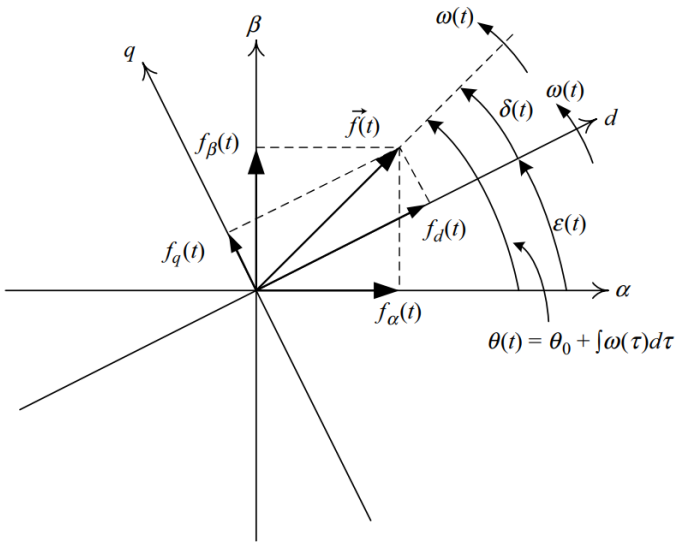


Figure 2: Difference Between *αβ-* and *dq-* frames

Core to designing controllers in *dq-frame* is the tracking of the frequency of the rotating phasor using a PLL [VSC]. The PLL controller diagram attached to its *Park transformer* is shown below in figure 3. The *q-axis* value is set to 0 since if $V_{sq} = \hat{V}_s \sin(\omega_o t + \theta_0 - \rho) = 0$, then $\sin(\omega_o t + \theta_0 - \rho) \approx (\omega_o t + \theta_0 - \rho)$ where $\hat{V}_s, \omega_o, \theta_o,$ and ρ corresponds to the q-axis magnitude of the phasor, frequency (in radians) of the phasor's rotation, and the frame shift in dq-frame respectively.

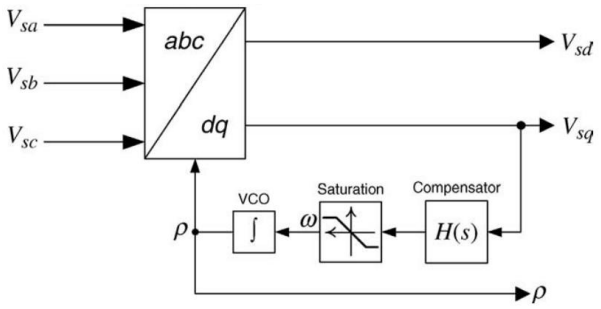


Figure 3: PLL connected to its Park Transformer

## II.B. Grid Following Inverters (GFLs)

IBRs in the form of GFLs inject P to the power grid based on MPPT. They are called *follower*s as they follow the grid's voltage and frequency as they inject power to the grid using PLL. Thus, GFLs are modelled as current sources [2] as shown below in figure 1.

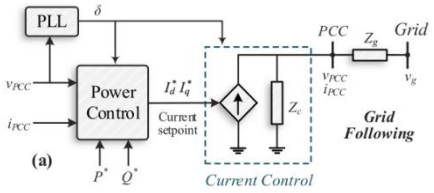


Figure 1: GFL modelled as Current Source [2]

The control block for GFLs is shown below in figure (a) which are essentially current controllers. By measuring the voltage on its terminals (or PCC when connecting to the grid), the power injected to the system at its output can referenced by the current injected since P=IV. Hence, given an input power signal, the appropriate reference current is the input for the controller shown below. Additional features such as third harmonic injection related blocks, DC bus voltage controllers can be added to improve performance and efficiency of the controller.

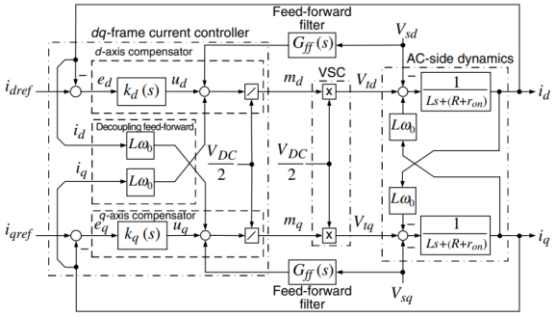


Figure (a): GFL control block: a current controller

Since GFLs follow the voltage and frequency on its PCC, any disturbance cannot be corrected by GFLs hence are more prone to instabilities. Although GFLs can be commanded to produce Q to help regulate voltage, from an economic point of view, GFLs are operated to inject P. Hence, GFLs causes frequency instability [2].

## II.C. Grid Forming Inverters (GFMs)

GFMs *form* its own voltage reference at its PCC and do not rely on PLL measurements and are modelled as voltage sources shown in figure 3. Thus, during disturbances, GFMs can self-synchronize hence offer more voltage and frequency stability. However, inertia is still important for frequency stability. Since GFMs are voltage sources, they show more similarities with synchronous generators. Also, GFMs allow for power sharing. Thus, GFMs can be controlled using frequency-based droop control or swing equation emulation.

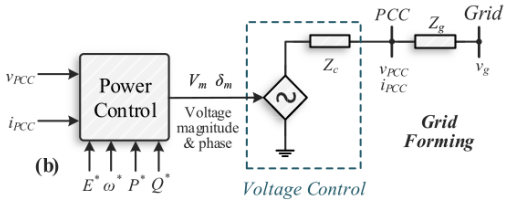


Figure 3: GFM modelled as Voltage Source [2]

The control diagram for GFMs is shown below in figure (b). Essentially, GFMs involve the controllers for GFLs however, the measurement is not from the grid but from the voltage formed by the GFM itself. Given an input voltage reference, the appropriate voltage output can be determined from the dynamics of the load. Due to the nature of GFMs' control blocks, GFMs are capable of both connecting to the grid to inject power or to form its own voltage reference during islanding. The high-level diagram is shown below in figure (c).

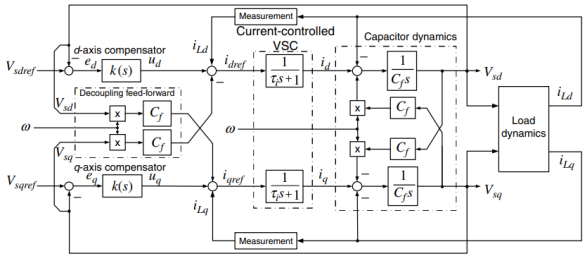


Figure (b): GFM Control Block Diagram

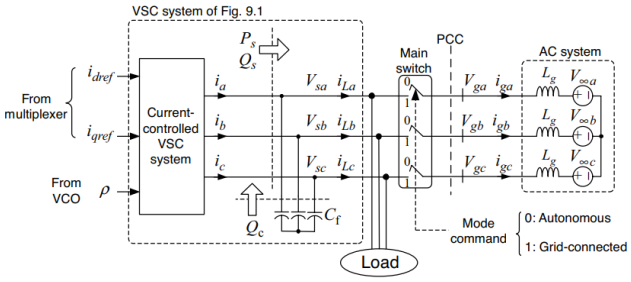


Figure (c): GFMs Autonomous and Grid Connected Mode Control

Due to GFM's similarities to a synchronous generator, GFMs are controlled to emulate a generators frequency and inertial response through droop control and swing equation control. Frequency-based droop control relates the frequency to change in power in a linear manner [2] with control diagram shown in figure 4. GFMs in this manner mimic the frequency characteristics of a synchronous generator [4].

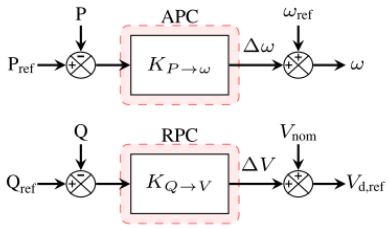


Figure 4: Frequency Droop Control Diagram [2]

Swing equation emulation on the other hand emulates the dynamics of a synchronous machine during disturbances based on the swing equation shown below. Figure 5 shows the control diagram of this control method. In this method, *virtual inertia* is produced to support grid stability.

$$J\omega_0 \frac{d\omega_r}{dt} + D_p\omega_r = P_m - P_e$$

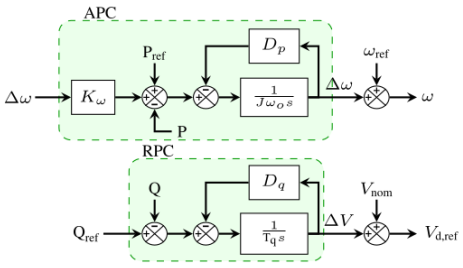


Figure 5: Swing Equation Emulation Control Diagram [2]

## II.D. Grid Strength and Duality of GFMs and GFLs

Based on the above discussion, GFMs show more promising characteristics than GFLs. However, related works suggest that the grid dynamics change drastically at high penetration grids where the traditional SCR definition of grid strength (defined by equation below) may not be accurate and outdated [3]. The traditional definition of grid strength relates to SCR which refers to voltage stiffness of the grid.

$$ECSR = \frac{1}{Z_{sys,pu}} = Y_{sys,pu}$$

[4] shows that GFMs and GFLs are dual. Based on ECSR, a strong grid needs low impedance. However, [4]'s results show that GFMs are unstable at low impedances while GFLs are stable. Thus, rethinking grid strength is imperative. Duality is indirectly supported by [5] which utilizes switching sequence of GFM-GFL control during disturbances. As proposed by [5], an IBR control method with GFM control to reduce frequency deviation then switching GFL to speed up settling time greatly utilizes the fast response of GFLs and frequency support of GFMs. Results of [5] show great improvement in frequency response in isolated power grids.

# III. METHODOLOGY

The analysis is conducted via simulations using PSCAD on the IEEE 14 bus system shown in figure 6. The GFM:GFL ratio is adjusted 20% at a time per scenario. The GFM and GFL models used are from the open-source generic Kenyon models from [6]. The Kenyon models only support frequency-droop support hence do not provide *virtual inertia*. Both GFMs and GLFs' set points are based on the specifications of the IEEE 14 bus system shown in table (a). Table 1 shows the placement of GFMs and GFLs per scenario.

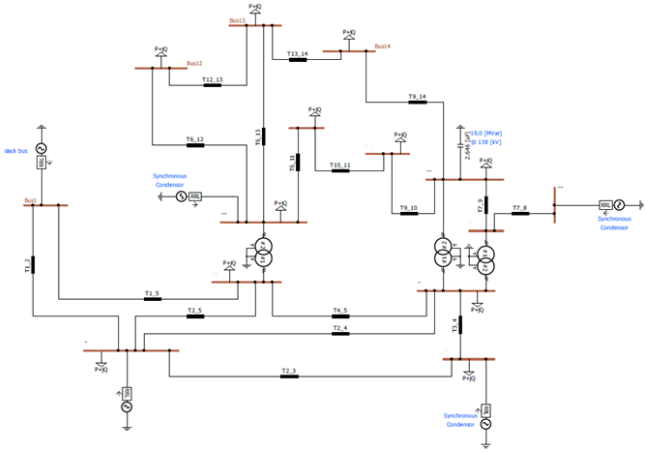

Figure 6: IEEE 14 Bus System in PSCAD

| Bus | V [kV] | Angle [deg] | P [pu] | Q [pu] |
|---|---|---|---|---|
| **1** | 146.28 | 0.0000 | 2.3239 | -0.1655 |
| **2** | 144.21 | -4.9826 | 0.4000 | 0.4356 |
| **3** | 138.38 | -12.7250 | 0.0000 | 0.2508 |
| **6** | 147.66 | -14.2209 | 0.0000 | 0.1273 |
| **8** | 150.42 | -13.3596 | 0.0000 | 0.1762 |

Table (a): IEEE 14 Bus Set Points

| | Simulation Cases for Load Increase (+5MW, +1MVAR / phase) and Faults | | | | | | Additional Cases for Faults | | |
|---|---|---|---|---|---|---|---|---|---|
| Generator | Base | 5:0 | 4:1 | 3:2 | 2:3 | 1:4 | N-2:3 | N-3:2 | N-4:1 |
| Bus 1 | IDEAL | GFM | GFM | GFM | GFM | GFM | GFM | GFM | GFM |
| Bus 2 | IDEAL | GFM | GFL | GFL | GFL | GFL | GFL | GFL | GFM |
| Bus 3 | IDEAL | GFM | GFM | GFM | GFL | GFL | GFM | GFM | GFM |
| Bus 8 | IDEAL | GFM | GFM | GFL | GFL | GFL | GFL | GFM | GFM |
| Bus 5 | IDEAL | GFM | GFM | GFM | GFM | GFL | GFL | GFL | GFL |

Table 1: GFM-GFL Configurations per Simulation

Five simulation sets are conducted: (1) load changes on highest power bus [bus 4], (2) load changes on random location [bus 5], (3) L-G fault [TL 6-11], (4) S-G fault [TL 6-11], and (5) L-G fault on highest power flow line [TL 1-2]. Analysis is conducted by measuring (1) frequency nadir, and (2) the slope between frequency nadir with respect to its nominal frequency (RoCoF: rate of change of frequency). Due to PSCAD license limitations, RoCoF is defined as a two-point slope instead of a continuous curve defined in [6].

# IV. RESULTS

Figure 7 below shows the frequency nadirs observed and figure 8 shows the average frequency nadirs and average RoCoFs for simulation set (1). Figure 9 shows the observed frequency nadirs and figure 10 shows average frequency nadirs and RoCoF values for simulation set (2). Figure 11 shows the frequency nadirs for a single-phase-to-ground fault on transmission line [TL 6-11] of simulation set (3) while figure 12 shows the average nadirs and RoCoFs. Figure 13 shows the frequency nadirs observed for simulation set (4) while figure 14 shows the average nadirs and RoCoFs. Finally, figures 15 and 16 show results for simulation set (5).

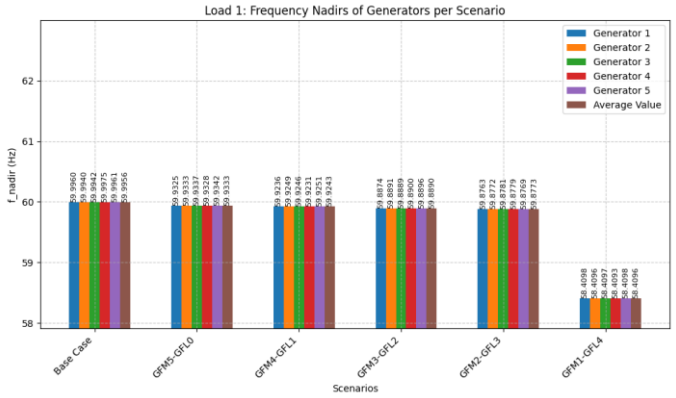


Figure 9: Observed Frequency Nadirs for Simulation set (1)

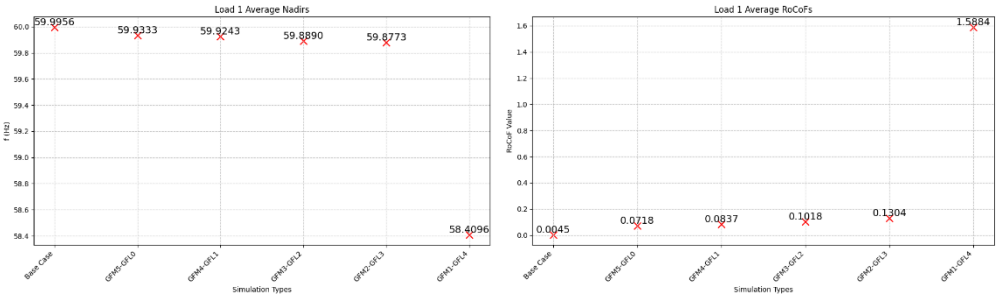


Figure 10: Simulation set (1) Average Frequency Nadirs and RoCoFs

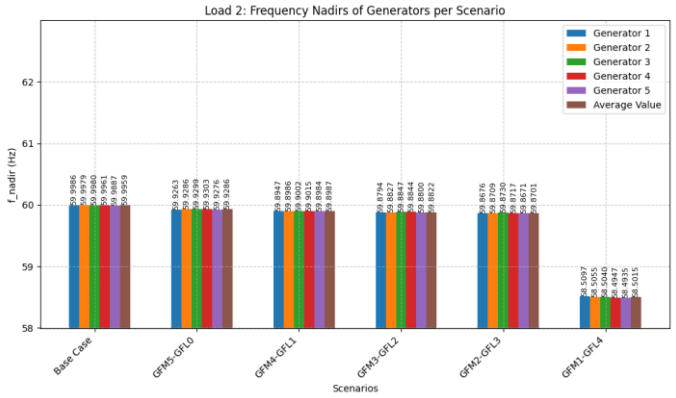


Figure 11: Observed Frequency Nadirs for simulation set (2).

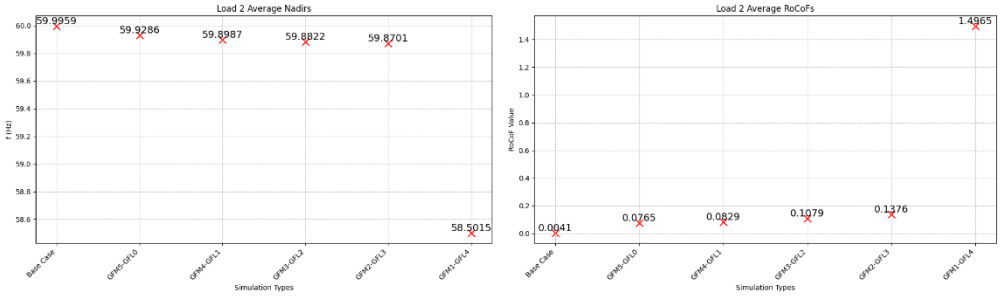


Figure 12: Simulation set (2) Average Frequency Nadirs and RoCoFs

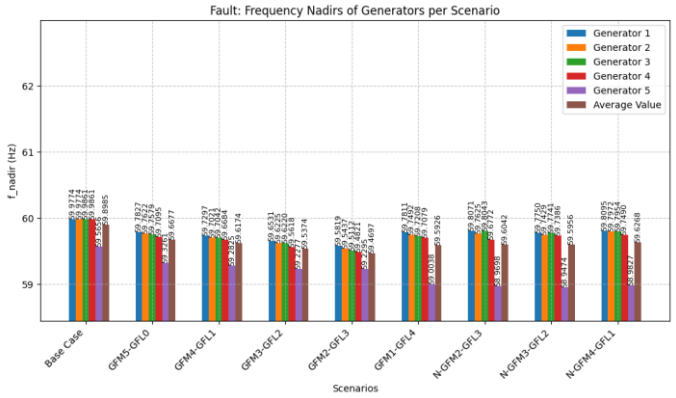


Figure 13: Observed Frequency Nadirs for simulation set (3)

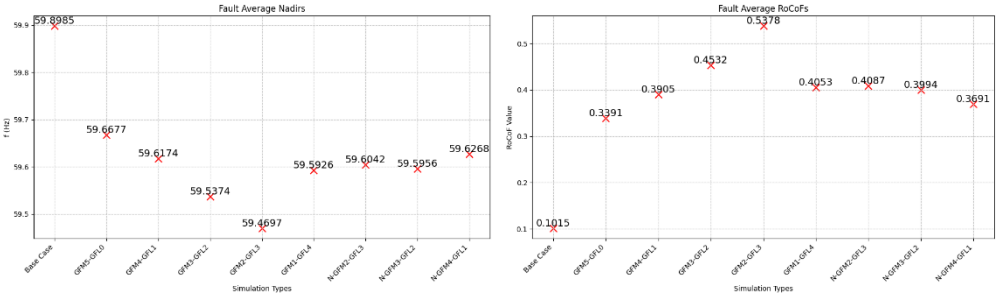


Figure 14: Simulation set (3) Average Frequency Nadirs and RoCoFs

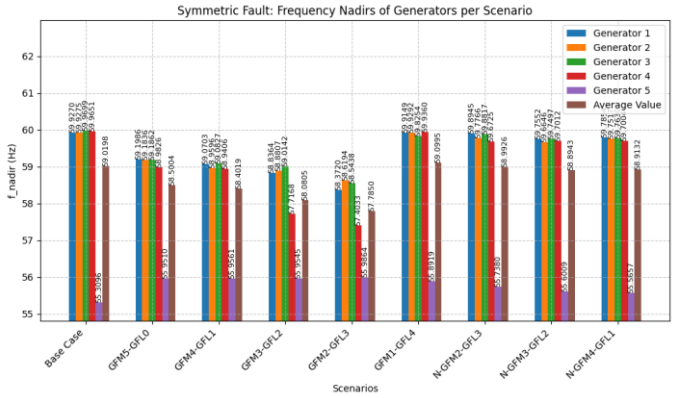


Figure 15: Observed Frequency Nadirs for simulation set (4)

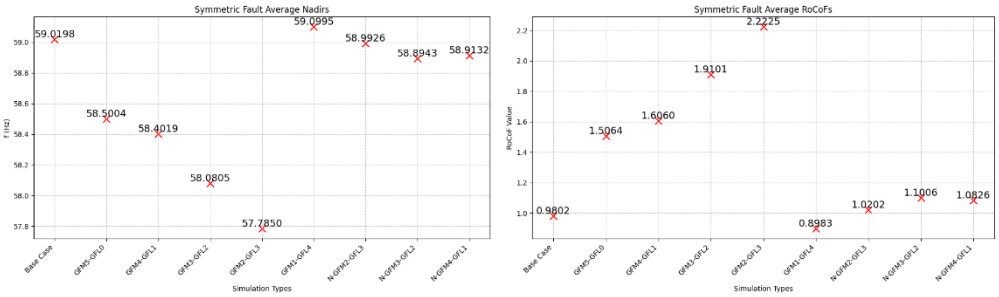


Figure 16: Simulation set (4) Average Frequency Nadirs and RoCoFs

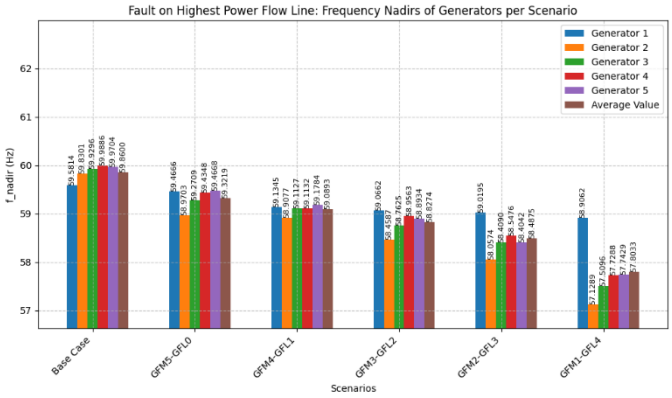


Figure 17: Observed Frequency Nadirs for simulation set (5)

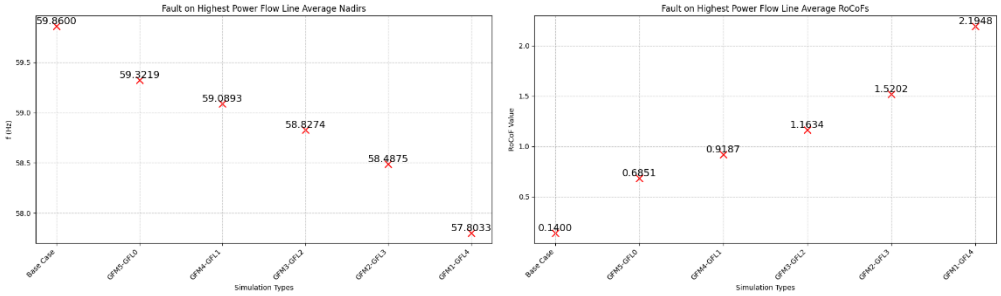


Figure 18: Simulation set (5) Average Frequency Nadirs and RoCoFs

# V. DISCUSSION

Results show that during load changes, frequency stays close to nominal until 1:4 ratio for both simulation sets (1) and (2). Although it may suggest that GFM:GFL ratio should be kept above 1:4, the simulation only has one GFM while all the GFLs power setting does remains constant. Hence, it can also be seen that the lone GFM bears all responsibility to compensate for the load increase. Nevertheless, it can be concluded that there should be enough GFMs to allow for power sharing to minimize potential overheads for the remaining active GFMs on the grid. The change in location for set (1) and (2) also implies that load changes *may* be independent to location in zero-inertia grids.

The results for the fault analysis show more promising results. For a simple fault, the average frequency nadir drops as number of GFMs decreases. However, if the fault occurs next to a GFL, the frequency dynamic is synonymous to a 4:1 GFM-GFL ratio. For symmetric faults, the results suggest the same conclusion – decrease in GFMs result in lower frequency stability. However, when the fault appears next to a GFL, the frequency response is synonymous to the ideal case which could be due to the small power set points of the GFLs; with slight improvements as GFMs increase. The same goes for set (5) wherein decrease in GFMs result in decreased frequency stability.

Based on the above discussion, the ratio of GFMs to GFLs should be kept as high as possible for stable frequencies during load changes to ensure low overhead per GFM during load sharing. For faults, GFM-GFL ratio stays relatively constant for 5:0 and 4:1 ratio. Hence, GFMs count should be at least 80% for good fault frequency stability.

# V. CONCLUSIONS

The frequency stability of different GFM-GFL ratios in zero inertia grids is analyzed through PSCAD simulations under load changes and faults. Based on the results, the higher the GFM ratio the better. If a threshold is to be set, an 80% GFM to 20% GFL ratio should be maintained to achieve consistent frequency stability. For load changes, a higher GFM ratio allows for more GFMs to participate in load sharing. For faults, a ratio above 4:1 result in similar frequency nadirs and RoCoFs between faults occurring next to GFLs and next to GFMs.

Surprisingly, faults occurring next to GFLs in the zero-inertia grid show consistent frequency response. In fact, the symmetric fault case for 1:4 ratio shows the least RoCoF and highest frequency nadir. Multiple repeats of the simulation were made to confirm if this was an error, however it was not. This somewhat agrees with the research papers on high-penetration grids that the grid dynamics change at high penetration. Further research needs to be conducted to fully understand this phenomenon, which is part of my future work.

The implication of this research concerns integration of IBRs to major grids in the future. Since it was shown that high GFM% allows for better frequency stability, electric power authorities must start using GFMs when installing new IBR systems to prepare the grid to become a high-penetration grid with GFM-GFL ratio above 4:1. For microgrids, a 100% GFM setting might be planned however allowing a few GFLs for cost reduction as long as it within 4:1 ratio can be an option of necessary.

# REFERENCES

[1] P. Denholm et. al. “Inertia and the Power Grid: A Guide without the Spin”, National Renewable Energy Laboratory, Golden, CO, Tech. Rep. NLEL/TP-6A20-73856

[2] D. B. Rathnayake et al., "Grid Forming Inverter Modeling, Control, and Applications," in IEEE Access, vol. 9, pp. 114781-114807, 2021, doi: 10.1109/ACCESS.2021.3104617.

[3] C. Henderson, A. Egea-Alvarez, T. Kneuppel, G. Yang and L. Xu, "Grid Strength Impedance Metric: An Alternative to SCR for Evaluating System Strength in Converter Dominated Systems," in IEEE Transactions on Power Delivery, doi: 10.1109/TPWRD.2022.3233455.

[4] Y. Li, Y. Gu and T. C. Green, "Revisiting Grid-Forming and Grid-Following Inverters: A Duality Theory," in IEEE Transactions on Power Systems, vol. 37, no. 6, pp. 4541-4554, Nov. 2022, doi: 10.1109/TPWRS.2022.3151851.

[5] W. Qiu et al., "A Grid Forming/Following Sequence Switching Control Strategy for Supporting Frequency Stability of Isolated Power Grids," 2023 5th Asia Energy and Electrical Engineering Symposium (AEEES), Chengdu, China, 2023, pp. 212-217, doi: 10.1109/AEEES56888.2023.10114155.

[6] R. W. Kenyon, A. Sajadi, A. Hoke and B. -M. Hodge, "Open-Source PSCAD Grid-Following and Grid-Forming Inverters and A Benchmark for Zero-Inertia Power System Simulations," 2021 IEEE Kansas Power and Energy Conference (KPEC), Manhattan, KS, USA, 2021, pp. 1-6, doi: 10.1109/KPEC51835.2021.9446243.